

## Dynamics of Photoexcited GaAs Band-Edge Absorption with Subpicosecond Resolution

C. V. Shank, R. L. Fork, R. F. Leheny, and Jagdeep Shah  
*Bell Telephone Laboratories, Holmdel, New Jersey 07733*

(Received 6 June 1978)

Time-resolved measurements of optically induced changes in the near-band-gap transmission spectrum of GaAs at 80°K, following excitation with an ultrashort laser pulse, provide a means of directly monitoring the hot-carrier distribution as it cools to the lattice temperature with a time constant of 4 psec. Exciton screening and band-gap renormalization are observed to occur in less than 0.5 psec.

Measurements of the time-resolved absorption spectrum in GaAs provide a unique means for directly observing the dynamics of an optically excited hot-carrier distribution as well as the influence of these carriers on exciton screening and renormalization of the band gap. Previously Shah, Leheny, and Wiegman<sup>1</sup> studied the influence of photoexcited carriers on the thermalized absorption spectrum of GaAs. Indirect measurements of hot-carrier energy relaxation rates using microwave<sup>2</sup> and optical techniques<sup>3-5</sup> have also been reported. In the present work we directly observe the hot-carrier distribution as it relaxes to the lattice temperature with a time constant of 4 psec and show that exciton screening and band-gap renormalization occur in less than 0.5 psec. It has been possible to measure these processes as a result of newly developed subpicosecond optical techniques.<sup>6</sup>

Absorption of photons with  $h\nu > E_g$  generates carriers with significant excess energy which relax to the band edge primarily by LO-phonon emission.<sup>7</sup> For GaAs this is an extremely rapid process and photoexcited carriers generated a few tenths of an eV above the band edge are expected to relax to within an LO-phonon energy ( $\hbar\omega = 37$  meV) of the band edge in less than a few tenths of a picosecond. Simultaneously, carrier-carrier scattering redistributes energy among the carriers and leads to a carrier distribution described by an effective temperature higher than the lattice temperature for sufficiently high carrier density.<sup>7</sup> By observing the time evolution of the transmission spectrum, the cooling rate for these carriers can be determined.

The capability of making spectral measurements with subpicosecond time resolution is the result of recent advances in subpicosecond optical-pulse generation. Subpicosecond pulses (0.5 psec) from a passively mode-locked dye laser operated at 6150 Å were cavity dumped at a 10-Hz rate. These pulses were amplified with a dye amplifier pumped by the frequency-doubled out-

put of a Nd:YAIG (neodimium-doped yttrium aluminum garnet) laser to powers of 200 MW. The output of the amplifier was divided to form two separate beams. The first beam was used to pump the sample after passing through a variable optical delay line driven by a stepper motor and then focused into a quartz cell containing ethanol which generated a Raman-shifted pulse at 7500 Å. The output was focused onto a 140- $\mu\text{m}$ -diam spot on the sample at an energy density of 3  $\mu\text{J}/\text{cm}^2$ . The second beam was focused into a cell containing water, generating a broadband subpicosecond continuum<sup>8</sup> which was used to probe the sample. Filters were used to select the spectral region of interest (7850–8350 Å) and to attenuate the beam to an energy density below that which altered the optical properties of the sample ( $5 \times 10^{-9}$  J/cm<sup>2</sup>). The probe pulses were imaged through the region of the sample excited by the pump pulses and onto the slits of a spectrometer. The spectrum transmitted by the spectrometer was detected by an optical multichannel analyzer (OMA) [Fig. 1(c)]. Transmission spectra were taken by averaging 300 pulses in the OMA for various delays between the pump and probe pulses. The transmission at selected wavelengths was also measured as a continuous function of the delay between pump and probe pulses. This was accomplished by driving the variable optical delay path with a stepper motor while recording the signal from a single channel of the OMA in a signal averager.

The sample consisted of a molecular-beam-grown layer of GaAs (1.5  $\mu\text{m}$  thick) supported by two layers of Al<sub>0.12</sub>Ga<sub>0.88</sub>As (2  $\mu\text{m}$  thick) which were transparent to both pump and probe wavelengths. The sample, mounted on a cold finger which was in contact with liquid N<sub>2</sub>, was maintained at a temperature of ~ 80°K.

The near-band-edge transmission spectra of the GaAs sample prior to optical pumping is shown in the trace for  $\tau < 0$  in Fig. 1(a). The spectra in Fig. 1 have been corrected for the

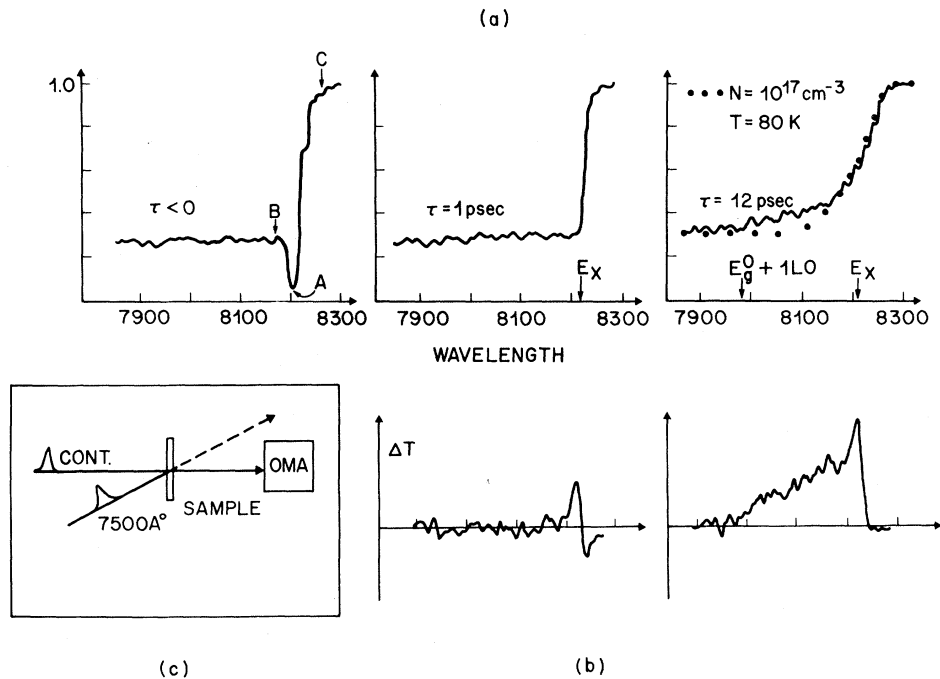


FIG. 1. (a) Transmission spectra corrected for wavelength variation of probe beam and OMA detector response. Spectra were recorded over a range of delay times between the pump and probe beams. (b) Difference spectra showing the difference between spectra obtained after a fixed delay and the spectra obtained for  $\tau < 0$ . These spectra were obtained by electronically subtracting the data stored in two memories of the multichannel analyzer. (c) Schematic of experiment. The OMA consisted of a spectrometer and an intensified silicon vidicon with multichannel signal averager.

spectral variation of the detector and probe beam and are believed to be accurate to  $\pm 10$  percent over the 85-meV range of the measurement. The sharp dip in transmission near  $8200 \text{ \AA}$ , due to the free-exciton absorption, is clearly resolved. The uniform absorption extending to shorter wavelengths results from band-to-band transitions and at longer wavelengths the sample is essentially transparent. Perturbed spectra [Fig. 1(a)] and difference spectra [Fig. 1(b)] are shown for delays of 1 and 12 psec following the excitation pulse. The difference spectra are obtained by electronically subtracting the unperturbed from the perturbed transmission spectra. These spectra more clearly illustrate the change in transmission.

A number of features are evident upon examination of these results. For the probe delayed 1 psec with respect to the pump [Fig. 1(a)], the sharp exciton resonance absorption has virtually disappeared. We attribute this change to a screening of the exciton by the photoexcited carriers.<sup>1,9,10</sup> In addition, the absorption edge has shifted to an energy just below the unperturbed

free-exciton energy, consistent with a renormalization of the band gap due to exchange and correlation effects between the carriers.<sup>11</sup> For a carrier density of  $n = 10^{17} \text{ cm}^{-3}$ , the band-edge shift due to these effects is expected to be 12 meV at low temperature<sup>1</sup> and may be less at higher temperatures. The difference spectrum illustrates these screening and renormalization effects, showing an increase in transmission at the exciton energy and a decrease at lower energy. For longer delays, the carriers lose additional energy and relax to states near the band edge. This results in a decrease in absorption at the band edge due to band-filling effects. This is illustrated in the trace for 12 psec where there is a significant change in transmission up to 20 meV above the unperturbed gap. Again, the difference spectrum provides a clear illustration of these effects. We have calculated the expected transmission spectrum for an equilibrium distribution of  $10^{17}\text{-cm}^{-3}$  carriers at 80 K including a 12-meV shift in the band gap and show the resultant spectrum as the dotted curve in Fig. 1(a).

A complementary picture of the dynamical

processes is obtained by scanning the time delay for a fixed wavelength. Continuous traces of the change in transmission with time are shown in Fig. 2. These traces were measured at the wavelengths labeled A, B, and C in Fig. 1(a). For A, corresponding to the free-exciton energy, the trace exhibits an initial rapid increase as the exciton is screened within the time resolution of the experiment (0.5 psec), and a more gradual increase as the carriers come into equilibrium with the lattice. We expect carrier screening to occur in a time on the order of the inverse carrier plasmon frequency (a few tenths of a picosecond for  $n = 10^{17} \text{ cm}^{-3}$ ) in agreement with our observation. At C, corresponding to the long-wavelength side of the free exciton, there is an initial fast decrease followed by a slow increase. We attribute these changes to the band-gap renormalization followed by band filling as the carriers relax. At B, on the short-wavelength side of the free exciton, band-gap renormalization does not affect the density of states significantly. We therefore attribute the relatively slow increase in transmission to the effects of band filling.

The time constant associated with the band-filling effects can be related directly to the carrier-energy relaxation. Initially the photoexcited carriers occupy states approximately 3 LO-phonon energies ( $\hbar\omega_{LO} = 37 \text{ meV}$ ) above the band edge. For carrier densities typical of our experimental conditions ( $n \sim 10^{17} \text{ cm}^{-3}$ ), carrier-carrier interactions can thermalize the carrier distribution in

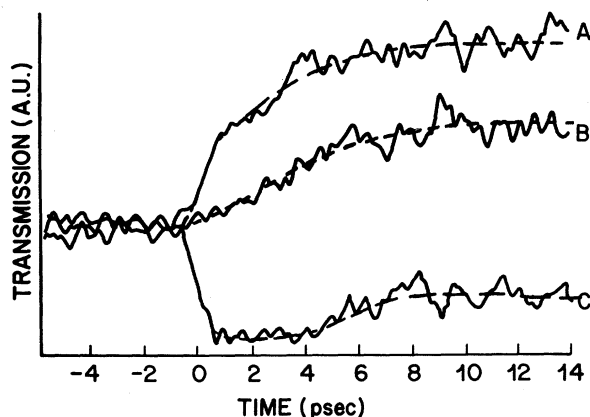


FIG. 2. Transmission at a fixed wavelength as a function of delay time. The three traces correspond to the wavelengths indicated in the  $\tau < 0$  trace of Fig. 1(a) and represent detailed time evolution at the three characteristic energies as described in the text.

a time short compared to our measurement time. Simultaneously LO-phonon emission by carriers occurs. As a result, at 1-psec delay, the carrier distribution corresponds to a thermalized distribution such that the average carrier energy is a significant fraction of the initial excess energy. The thermalized carrier distribution continues to cool to the lattice temperature by further interactions of the carriers with the lattice, with carrier-carrier interactions maintaining a well-defined carrier temperature. For the case of GaAs with carrier temperatures  $\geq 40^\circ\text{K}$ , LO-phonon emission by the fraction of carriers with energy greater than  $\hbar\omega_{LO}$  dominates this cooling, and the rate of cooling by this mechanism is given for GaAs<sup>7</sup> by  $dE/dt \approx 10^{-7} [\exp(x_0 - x_e) - 1] / [\exp(x_0) - 1] \text{ J/sec}$ , where  $x_i = \hbar\omega_{LO} / kT_i$  with  $T_i$  the electron (e) or lattice (0) temperature. The rate depends on the carrier temperature, but can be numerically integrated to determine the time required to cool from one temperature to another. We have calculated the time required to cool the carrier distribution for GaAs for our experimental condition to be 3 psec, in good agreement with the 4-psec time constant observed for the slow rise in the transmission.

In summary, time-resolved measurements of the absorption spectrum following injection of optically excited hot carriers have revealed that screening of the free exciton and a shift in the band edge occur in less than 0.5 psec. In addition, the hot-carrier distribution approaches the lattice temperature with a time constant of approximately 4 psec. A study of the temperature dependence of the carrier equilibration rate is contemplated for future work.

The authors acknowledge the assistance of R. Dingle in obtaining samples and discussions with T. M. Rice.

<sup>1</sup>J. Shah, R. F. Leheny, and W. Wiegmann, *Phys. Rev. B* **15**, 1577 (1977).

<sup>2</sup>K. Seeger, in *Electronic Materials*, edited by N. B. Hannay and U. Colombo (Plenum, New York, 1973), Chap. 5.

<sup>3</sup>C. V. Shank, D. H. Auston, E. P. Ippen, and O. Teschke, to be published; D. H. Auston, S. McAfee, C. V. Shank, E. P. Ippen, and O. Teschke, *Solid State Electron.* **21**, 147 (1978).

<sup>4</sup>R. G. Ulbrich, *Phys. Rev. B* **8**, 5719 (1973).

<sup>5</sup>R. G. Ulbrich, *Solid State Electron.* **21**, 51 (1978).

<sup>6</sup>E. P. Ippen and C. V. Shank, in *Topics in Applied Physics*, edited by S. L. Shapiro (Springer-Verlag,

New York, 1977), Vol. 18, p. 83.

<sup>7</sup>J. Shah, *Solid State Electron.* **21**, 43 (1978).

<sup>8</sup>See chapter by D. H. Auston, in *Topics in Applied Physics*, edited by S. L. Shapiro (Springer-Verlag, New York, 1977), Vol. 18.

<sup>9</sup>J. G. Gay, *Phys. Rev. B* **4**, 2567 (1971).

<sup>10</sup>J. D. Dow, in *Proceedings of the Twelfth International Conference on the Physics of Semiconductors*, edited by M. H. Pilkuhn (B. G. Teubner, Stuttgart, 1974), p. 957.

<sup>11</sup>W. F. Brinkman and T. M. Rice, *Phys. Rev. B* **7**, 1508 (1973).

## Electronic and Spin Structure of UTe

M. Erbudak

*Laboratorium für Festkörperphysik, Eidgenössische Technische Hochschule, 8093 Zürich, Switzerland*

and

J. Keller<sup>(a)</sup>

*Institut für Theoretische Physik, Eidgenössische Technische Hochschule, 8093 Zürich, Switzerland*

(Received 13 September 1978)

A self-consistent cellular multiple-scattering technique is used to calculate the density of states of uranium telluride. The  $5f$  band is found to be highly polarized and energetically localized although presenting enough itinerant character to keep its position at the Fermi level. The material shows a coupling between the  $5f$  and  $6d$  states. This interaction explains the observed negative spin polarization from photoelectrons up to 7 eV above the phototreshold.

Negative spin polarization of photoemitted electrons from magnetic materials, i.e., with electron magnetic moments antiparallel to the bulk magnetization and the externally applied field, has been of considerable interest. It was observed in ferromagnetic nickel<sup>1</sup> where it is compatible with both the atomic model of a more-than-half-full shell as well as with the band model in the case of nearly full bands. The occurrence of negative electron spin polarization (ESP) is restricted to within a spectral range of 80 meV from the Fermi level ( $E_F$ ),<sup>1</sup> which is the order of the smallest Stoner excitation in ferromagnetic nickel. For ferrimagnetic magnetite,  $\text{Fe}_3\text{O}_4$ , the negative ESP was observed also in a small energy range within  $E_F$ . It has been explained by the model of single ion in a crystal field, originating from  $\text{Fe}^{2+}$  ions in octahedral sublattices which are coupled antiferromagnetically to the rest of the crystal.<sup>2</sup> Hence, it is a structural property. Recently, the measurements of ESP from ferromagnetic UTe have shown a negative polarization throughout a spectrum of 7 eV below  $E_F$ .<sup>3</sup> The first attempts to interpret this observation assumed that the  $6d$ -electron magnetic moments were antiparallel to the crystal magnetization with the  $5f$ 's not being observed at low photon energies ( $h\nu < 11.0$  eV) due to vanishing matrix elements. Here, we re-

port a theoretical analysis based on a self-consistent cellular multiple-scattering technique. As a major result, it was found that it is not the nature of the  $6d$  electronic states alone which are responsible for the observed negative ESP, but the  $5f$  resonances located near  $E_F$  influencing the  $6d$ -electron density of states ( $d$ -DOS) in favor of the minority spins and thus creating a trough in the  $d$ -DOS of the majorities near phototreshold. By virtue of this  $f$ - $d$  interaction, the observed ESP is negative, since, as stated earlier, the  $5f$  electrons' contribution to the measured spectra can be taken as negligible.

Usually, the highly localized  $f$ -level eigenvalues show a large dependence on occupation. It is necessary to study  $f$ -band materials with methods which can treat localized or itinerant levels on equal footing. The method should also be practical for performing a large number of calculations with different assumed configurations in order to find self-consistently the occupation of the different bands. A self-consistent cellular one-electron-Green's-function technique for a finite cluster in condensed-matter-like boundary conditions presents these characteristics.<sup>4</sup>

In the multiple-scattering calculation the local density of states for the atomic species  $i$  at energy  $E$  is given by the integration over the cell